

Are there broad absorption-line blazars?

Sapna Mishra^{1,2*}, Gopal-Krishna¹, Hum Chand¹, Krishan Chand¹, Vineet Ojha¹

¹*Aryabhata Research Institute of Observational Sciences (ARIES), Manora Peak, Nainital – 263002, India*

²*Department of Physics & Astrophysics, University of Delhi, Delhi 110 007*

Accepted —. Received —; in original form —

ABSTRACT

We report the first systematic search for blazars among broad-absorption-line (BAL) quasars. This is based on our intranight optical monitoring of a well-defined sample of 10 candidates selected on the criteria of a flat spectrum and an abnormally high linear polarization at radio wavelengths. A small population of BAL blazars can be expected in the ‘polar model’ of BAL quasars. However, no such case is found, since none of our 30 monitoring sessions devoted to the 10 candidates yielded a positive detection of intra-night optical variability (INOV), which is uncharacteristic of blazars. This lack of INOV detection contrasts with the high duty cycle of INOV observed for a comparison sample of 15 ‘normal’ (i.e., non-BAL) blazars. Some possible implications of this are pointed out.

Key words: galaxies: active – galaxies: photometry – galaxies: jet – quasars: broad absorption line – (galaxies:) BL Lacertae objects: blazars – (galaxies:) quasars: broad absorption line

1 INTRODUCTION

Blue-shifted broad absorption-line (BAL) troughs seen in the optical/UV spectra (Weymann et al. 1991) of ~20% of QSOs are interpreted as the covering factor of the BAL outflow in the orientation based models, or as the duration of BAL phase, in a QSOs life in the evolutionary models (e.g., Pâris et al. 2012, and references therein). The outflow speed is found to be as high as 0.3c (e.g., Hamann et al. 2018). In ~ 1/7th of BALQSOs, the thermal plasma outflow is accompanied by ejection of a pair of relativistic plasma jets which can extend to kpc scale (Becker et al. 2000). Inferring the orientation of the jet axis from the spectral/structural radio properties as a statistical indicator has revealed no preference between the postulated equatorial (Cohen et al. 1995; Goodrich & Miller 1995; Murray et al. 1995; Elvis 2000; Proga et al. 2000) and polar (Punsly 1999; Becker et al. 2000; Zhou et al. 2006; Ghosh & Punsly 2007; Doi et al. 2009) configurations for the BAL outflows (see, e.g., Jiang & Wang 2003; Brotherton et al. 2006; Gregg et al. 2006; Bruni et al. 2013; Kunert-Bajraszewska et al. 2015). Although, both configurations may conceivably exist in a single BALQSO (e.g., Brotherton et al. 2006; Yang et al. 2012), the polar configuration would have a more direct bearing on the relativistic jet, given the likelihood of a physical interaction between the

outflowing BAL clouds and the jet on the inner parsec scale. Since the radio flux of such compact relativistic jets, when pointed near the line of sight, would appear strongly Doppler boosted, the polar outflows of absorbers should be frequently observed in those BALQSOs whose radio spectrum is flat or inverted, and this indicator has been employed in several studies (Becker et al. 2000; Montenegro-Montes et al. 2008; Bruni et al. 2012). Additional examples of such BALQSOs with aligned jets have been found through radio flux variability (Zhou et al. 2006; Ghosh & Punsly 2007; Montenegro-Montes et al. 2008; Doi et al. 2009).

Interestingly, Fanaroff-Riley type II radio morphology is ~ 10 times rarer among BAL quasars, compared to normal quasars in the Sloan Digital Sky Survey (SDSS) (see Gregg et al. 2006). The core dominated flat-spectrum sub-population of radio-loud quasars, called FSRQs, has a subset, namely blazars, which is characterised by parsec-scale relativistic jets of strongly Doppler boosted nonthermal radiation often showing superluminal motion, in addition to rapid flux variability and a strong ($p_{opt} > 3\%$) optical polarization which is highly variable (e.g., Fugmann 1988; Lister & Smith 2000). Another well established exceptionality to blazars is their strong intra-night optical variability (INOV), of amplitude $\psi > 3-4\%$ with a duty cycle of around 40-50% (Gopal-Krishna & Wiita 2018, and references therein). This opens up the possibility to confirm the blazar nature of the BAL quasars which are known to exhibit at least some radio properties that are commonly associated

* E-mail: sapna@aries.res.in(SM)

with blazars and hence may be regarded as manifestations of the polar model of the BAL phenomenon mentioned above. Here we shall apply the INOV test to a well-defined sample of 10 radio-loud BALQSOs exhibiting blazar signatures, namely a flat/inverted radio spectrum and a large radio polarization that locates them in the high polarisation tail for BAL quasars (optical polarimetric data on radio-loud BALQSOs being even scarcer, at present). This selection process makes our sample particularly suited for making a search for ‘BAL-blazars’, in contrast to a previous INOV search which was focussed on BAL quasars selected on the criterion of radio loudness alone and was found to show only a muted INOV (unlike blazars, e.g. see, [Joshi & Chand 2013](#)).

2 THE SAMPLE OF BAL-BLAZAR CANDIDATES

Our sample of 10 BAL-blazar candidates for intranight optical monitoring was derived from 6 publications reporting 56 radio detected BALQSOs (Table 1). Out of these, we have selected all 10 sources which have a positive declination, an SDSS-r band apparent magnitude, $m_r < 19$, a flat or inverted radio spectrum (i.e., $\alpha > -0.5$, [Becker et al. 2000](#)) and a radio (linear) polarization $p_{rad} > 3\%$ (Table 1). The choice of the $p_{rad} = 3\%$ threshold is based on the distribution of median fractional polarization of the radio core, measured for 387 AGNs, by multi-epoch VLBI at 15 GHz (figure 1 in [Hodge et al. 2018](#)). This distribution consists of a single large bump peaking at $p_{rad}(15 \text{ GHz}) = 1.5\%$, followed by a sharp drop setting in at $p_{rad}(15 \text{ GHz}) \sim 3.0\%$, and finally culminating in a low-amplitude tail which extends up to $p_{rad}(15 \text{ GHz}) = 9\%$. This high polarization tail of FSRQs is strikingly similar to the distribution of $p_{rad}(15 \text{ GHz})$ found for BL Lacs, which is plotted in the same figure 1 ([Hodge et al. 2018](#)) and for which the median value of $p_{rad}(15 \text{ GHz}) = 3.5\%$. Hence, it seems reasonable to expect that at least some of the flat-spectrum BAL quasars falling within the high polarization tail would turn out to be the putative BAL-blazars.

3 INTRANIGHT PHOTOMETRIC MONITORING

Photometric monitoring of each of our 10 BAL-blazar candidates was performed on 3 nights, adding up to a total of 30 intra-night monitoring sessions (details in the online tables 1 and 2). For 25 of the 30 sessions we used the 1.3-meter Devasthal Fast Optical Telescope (DFOT), equipped with a Peltier-cooled Andor CCD camera which has 2048×2048 pixels of $13.5 \mu\text{m}$ size, providing 18 arcmin field-of-view (FoV) on the sky ([Sagar et al. 2011](#)). For another 3 sessions the 1.04 meter Sampurnanand Telescope (ST) was used, which is equipped with a 1340×1300 pixel liquid-nitrogen cooled PyLoN CCD of 20-micron pixel size, providing a 6.8×6.5 arcmin FoV ([Sagar 1999](#)). Monitoring in the remaining 2 sessions was carried out with the 2.0-meter Himalayan Chandra Telescope (HCT) equipped with a 2148×2048 cryogenically cooled CCD detector covering a 10×10 arcmin FoV ([Prabhu & Anupama 2010](#)). Each target AGN

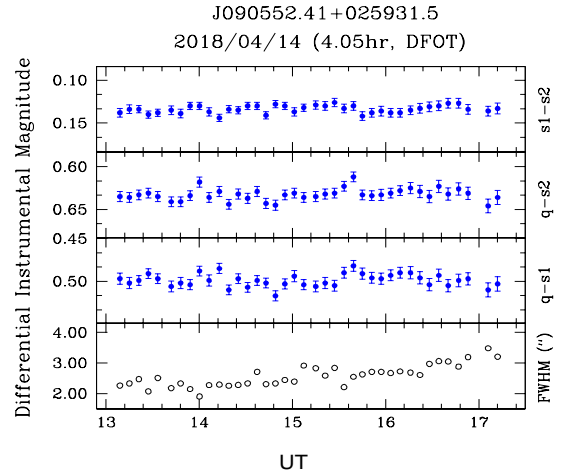


Figure 1. An example of the DLCs obtained in the present study. The target AGN is the BAL quasar J090552.41+025931.5. DLCs for all the 30 sessions are presented in online figure 1. The date and duration of monitoring and the telescope used are mentioned at the top. The profile in the upper panel presents the DLC of the chosen two comparison stars (“star-star” DLC). The two middle profiles display the DLCs of the BAL quasar relative to the two comparison stars, as mentioned in the labels on the right side. The profile in the bottom panel shows the variation of the seeing disk (FWHM) through the monitoring session.

(BAL-blazar candidate) was monitored in 3 separate sessions continuously for a minimum duration of 3-hours, in a sequence of 5-10 minute long exposures. At least 2 or 3 comparison stars were also recorded on each CCD frame, enabling differential photometry of the target AGN relative to the comparison stars which were chosen *a priori* on the basis of their proximity to the AGN, both in apparent magnitude and the location on the CCD chip (online table 1).

Preliminary image processing (bias subtraction, flat-fielding, and cosmic-ray removal) was performed using the standard packages in IRAF¹. Aperture photometry was carried out using the task DAOPHOT II (Dominion Astrophysical Observatory Photometry software, [Stetson 1987](#)). Signal-to-noise ratio was found to peak for a photometric aperture radius nearly 2 times the seeing disc whose FWHM was determined by averaging the profiles of 5 fairly bright, unsaturated stars recorded in the same CCD frame. The measured instrumental magnitudes were then used to derive the ‘differential light curves’ (DLCs) of the target AGN relative to two (steady) comparison stars, as well as the star-star DLC for the session (see [Goyal et al. 2013](#), for details of the procedure). In Fig. 1, we show the differential light curves (DLCs) obtained from one of the 30 sessions; the DLCs for all 30 monitoring sessions are presented in the online figure 1.

¹ Image Reduction and Analysis Facility, distributed by NOAO, operated by AURA, Inc. under agreement with the US NSF.

Table 1. The sample of 10 BAL–blazar candidates monitored for intranight optical variability (INOV).

Source name	RA (J2000)	DEC (J2000)	z_{em}	AI	m_r	$S_{1.4GHz}$	S_{150MHz}	L_{150MHz}	α_{radio}	Log(R)	Fractional polarisation % (at GHz)	Ref. codes
SDSS (1)	hh:mm:ss (2)	°:':" (3)	(4)	(kms^{-1}) (5)	(6)	mJy (7)	mJy (8)	erg/s/Hz (9)	(10)	(11)	(12)	(13)
J090552.41+025931.5	09:05:52.41	+02:59:31.5	1.82	130	16.91	35.6	46.80	1.07×10^{34}	0.12	1.76	7.7 ± 3.8 (1.4)	d,f
J092824.13+444604.7	09:28:24.13	+44:46:04.7	1.90	293	18.31	166.5	73.60	1.89×10^{34}	-0.36	2.80	4.6 ± 0.7 (1.7)	c,e
J092913.97+375743.0	09:29:13.97	+37:57:43.0	1.91	2170	18.04	42.7	125.30	3.24×10^{34}	0.48	2.20	6.1 ± 0.9 (1.4)	d,f
J105416.51+512326.1	10:54:16.51	+51:23:26.1	2.34	2220	18.73	34.8	74.10	3.14×10^{34}	0.34	2.38	4.2 ± 1.1 (1.4)	d,f
J115944.82+011206.9	11:59:44.82	+01:12:06.9	2.00	2887	17.27	271.1	331.10	9.57×10^{34}	0.09	2.60	6.5 ± 1.7 (1.4)	c,b,e
J123717.44+470807.0	12:37:17.44	+47:08:07.0	2.27	1300	18.58	89.2	50.30	1.98×10^{34}	-0.26	2.47	5.9 ± 2.6 (8.46)	d,f
J131213.57+231958.6	13:12:13.57	+23:19:58.6	1.51	-	17.32	45.8	67.90	0.98×10^{34}	0.18	1.88	3.6 ± 2.3 (22)	b
J140653.84+343337.3	14:06:53.84	+34:33:37.3	2.56	350	18.72	165.3	150.00	7.91×10^{34}	-0.04	2.83	3.5 ± 0.2 (8.46)	d,f
J162453.47+375806.6	16:24:53.47	+37:58:06.6	3.38	1020	18.45	54.6	35.60	3.67×10^{34}	-0.19	2.41	11.3 ± 1.5 (22.46)	a,b,d,f
J162559.90+485817.5	16:25:59.90	+48:58:17.5	2.72	-	18.09	25.8	<7.00	0.55×10^{34}	-0.47	1.90	17.6 ± 14.0 (43)	b

Notes. Col. 1: source name; Col. 2,3: coordinates; Col. 4: emission redshift; Col. 5: absorption index (Hall et al. 2002); Col. 6: r-band magnitude from SDSS; Col. 7: peak flux density at 1.4 GHz; Col. 8,9: peak flux density and luminosity at 150 MHz; Col. 10: spectral index ($f_\nu \propto \nu^\alpha$) between 150 MHz and 1.4 GHz; Col. 11: radio loudness parameter $R = f_{5\text{GHz}}/f_{2500\text{\AA}}$; Col. 12: fractional polarization (frequency); Col. 13: reference code(s).

References: (a) Benn et al. (2005); (b) Montenegro-Montes et al. (2008); (c) Doi et al. (2009); (d) Bruni et al. (2012); (e) Hayashi et al. (2013); (f) Bruni et al. (2015).

4 STATISTICAL ANALYSIS AND RESULTS

Following Goyal et al. (2013), we applied the widely used F^η test to the DLCs of the target AGN relative to the two comparison stars (s_1, s_2). The parameter F^η computed for the two AGN DLCs, is defined as:

$$F_j^\eta = \frac{\text{Var}(q - s_j)}{\eta^2 \langle \sigma_{err}^2 \rangle}; \quad \langle \sigma_{err}^2 \rangle = \sum_{i=1}^N \sigma_{i,err}^2 (q - s_j) / N \quad (1)$$

Here $\text{Var}(q - s_j)$ is the variance of the ‘AGN– j^{th} comparison star’ DLC, where $j=1,2$ and $\sigma_{i,err}(q - s_j)$ are the photometric error of the N individual data points in the DLC (as returned by the DAOPHOT routine). For each of the two DLCs, $i=1$ to N and $\eta = 1.5$ (see Goyal et al. 2012).

For each of the two DLCs of the target AGN, online table 2 (Column 7) compares the computed values of F^η with the critical value of F ($= F_c^\alpha$). The values of α are set at 0.05 and 0.01, corresponding to 95% and 99% confidence levels for INOV detection. If the computed F^η for a DLC exceeds F_c^α , the null hypothesis (i.e., no variability) is rejected at the corresponding confidence level. We thus classify a DLC as variable (‘V’) if its computed $F^\eta > F_c(0.99)$; probably variable (‘PV’) if the F^η lies between $F_c(0.95)$ and $F_c(0.99)$, and non-variable (‘NV’) in case $F^\eta < F_c(0.95)$ (Goyal et al. 2013). Column 10 in the online table 2 lists the session averaged photometric accuracy of the measured differential magnitudes $\sqrt{\eta^2 \langle \sigma_{err}^2 \rangle}$. It is estimated using the two AGN–star DLCs and is nearly always better than 3% (median = 2.0%).

5 DISCUSSION AND CONCLUSION

The main result from this study (online table 2) is the non-detection of INOV in any of the 30 sessions devoted to the present representative sample of 10 BAL–blazar candidates, selected on the basis of a flat/inverted spectrum and high linear polarization at centimeter/decimeter wavelengths (Table 1). We shall now compare this result with the INOV results reported in Goyal et al. (2013) for a sample of 24 ‘normal’ (i.e., non-BAL) blazars that were monitored in 85 sessions, also in red filter and subjected to the same F^η test. For this, we first need to extract an appropriate comparison sample out of those 85 sessions, in order to minimise the difference in sensitivity achieved for that and the present sam-

ple of DLCs. The monitoring for the present sample has been almost entirely performed using the 1.3-m DFOT (Sect. 3), whereas the 24 normal blazars were mostly monitored with the 1.04-meter ST.

Considering this, we adopt the premise that a proper comparison sample of DLCs of the normal blazars should be formed by matching in terms of the rms error found for the (non-varying) ‘star–star’ DLC for a given session. Thus, for the present sample of 30 DLCs of the 10 BAL–blazar candidates, we have built a comparison sample of 28 DLCs pertaining to 15 normal blazars, out of the Goyal et al. (2013) sample, adopting a tolerance of $\pm 0.5\%$ in the rms error mentioned above.

Using the data provided in table 1 of Goyal et al. (2013) we have computed the INOV duty cycle (DC) for the sample of ‘n’ DLCs of normal blazars, as:

$$DC = 100 \frac{\sum_{i=1}^n K^i (1/T_{int}^i)}{\sum_{i=1}^n (1/T_{int}^i)} \text{percent} \quad (2)$$

where $T_{int}^i = T_{obs}^i (1 + z_{em})^{-1}$ is the intrinsic rest frame monitoring duration corrected for the cosmological redshift, z_{em} . K^i was taken as 1 for a positive detection of INOV in the i^{th} session, otherwise, it was set to zero. We thus find, the INOV DC to be 41.2% for the comparison sample (28 sessions devoted to 15 normal blazars). This high value is in striking contrast to the non-detection of INOV in any of the 30 sessions devoted to our sample of 10 BAL–blazar candidates.

We now examine the possibility that the strong contrast between the INOV duty cycles found here between the samples of BAL–blazar candidates and normal blazars might arise from the systematic difference between their optical luminosities and/or redshifts (Fig. 2(a), Fig. 2(b)). To check the possible role of luminosity, we turn to the Goyal et al. (2013) sample of 85 DLCs of 24 normal blazars and divide it into two luminosity bins separated in absolute magnitude in B-band (M_B) at $M_B = -25.0$. The higher luminosity (high-L) bin contains 8 normal blazars monitored in 40 sessions and the lower luminosity (low-L) bin contains 16 normal blazars (45 sessions). For a proper comparison between these two sets of sessions, we again apply the aforementioned filter of rms matching to within a tolerance of $\pm 0.5\%$. This led to 37 sessions (8 blazars) from the high-L bin matching in the rms error with 37 sessions (16 blazars) of the low-L bin. The corresponding median M_B for these two lu-

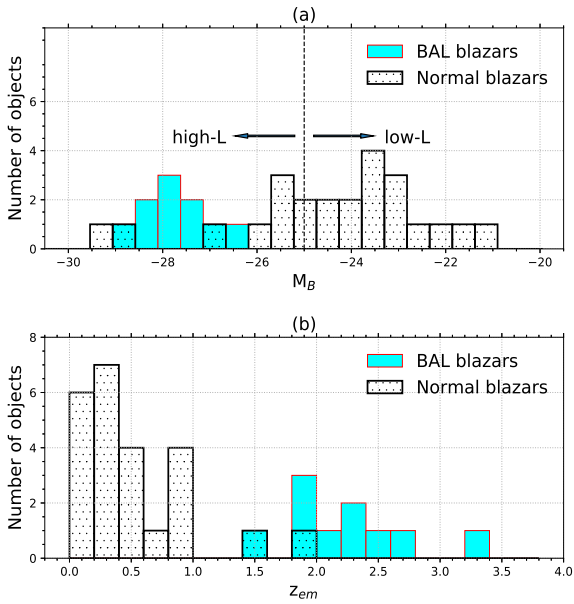


Figure 2. Distribution of absolute magnitude in B-band (M_B , upper panel) and emission redshift (lower panel) for the present sample of 10 BAL–blazar candidates (cyan filled) and for the sample of 24 normal blazars from Goyal et al. (2013) (black dotted). The dotted vertical in the upper panel corresponds to $M_B = -25.0$

minosity bins are -25.4 and -23.7 , respectively. Following Eq. 2 we have computed the INOV duty cycles and find them to be 44.5% and 52.0% for the high and low luminosity bins, respectively. Based on this, any decrement of DC with luminosity appears to be marginal. Could the marked contrast between the INOV of the BAL–blazar candidates and normal blazars then be because of the redshifts of the BAL–blazar candidates being systematically higher than those of the comparison sample of normal blazars described above (median redshifts of the two samples are 2.13 and 0.42)? An important consequence of this difference is that, when translated to the rest-frame, the intranight monitoring durations (T_{int}) are substantially shorter for the sample of BAL–blazar candidates. To seek a clue on this point, we again turn to the afore-mentioned Goyal et al. (2013) sample of 85 intranight monitoring sessions devoted to 24 normal blazars. We divide this dataset into 4 bins of T_{int} , each containing close to 20 sessions. Median values of T_{int} for these bins are 3.0, 4.0, 4.8 and 5.6 hr (Fig. 3). Computation of INOV DC for these 4 bins (Eq. 2) gives INOV DCs of 44.9%, 47.4%, 50.2%, and 56.5%, respectively (note that each of these estimates is the average of the DCs calculated for the two DLCs of a given AGN, derived relative to the two comparison stars). It is seen that even for the shortest bin of T_{int} (median = 3.0 hr) the INOV duty cycle is 44.9%, which is only marginally lower than the DCs found for the 3 bins of longer duration. Furthermore, there is little evidence that strong INOV is a rarer occurrence in sessions of shorter intrinsic duration (at least over this range of T_{int}). From Fig. 3 it is seen that for the shortest bin (with median = 3.0

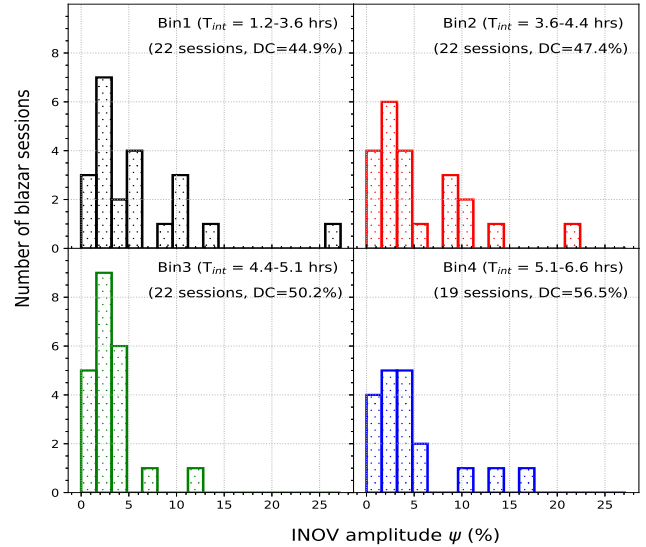


Figure 3. Distribution of INOV amplitude (ψ) for the 4 bins of T_{int} , derived using the comparison sample of 24 normal blazars monitored in 85 sessions (see text).

hr), strong INOV with amplitude $\psi \gtrsim 10\%$ was detected in 5 out of 22 sessions, which is evidently not smaller than the corresponding value (7/63) found for the aggregate of the 3 bins of longer sessions.

Thus, in order to reconcile the foregoing analysis with the present non-detection of INOV for the BAL–blazar candidates in any of the 30 sessions (median $T_{int} = 1.2$ hr) one might postulate a drastic drop in INOV strength for $T_{int} \lesssim 1-2$ hrs. Although, such a hypothesis cannot be ruled out at present (see, e.g., Romero et al. 2002; Gopal-Krishna et al. 2011; Gopal-Krishna & Wiita 2018), and it remains observationally verifiable, the alternative possibility that the non-detection of INOV for the BAL–blazar candidates could either undermine the polar model for the BAL outflows (Sect. 1), or be traceable to some other physical effect associated with that model. For instance, could it be that, as compared to normal blazars, physical conditions in the relativistic jets of BAL quasars are less conducive for strong INOV (as, for example, is their propensity to be incapable of developing FR II radio structures, e.g. see, Gregg et al. 2006). Origin of INOV has been associated with a zone of turbulence within a parsec-scale jet, just upstream of a relativistic shock, as sketched in Marscher et al. (2008) (see, also, Goyal et al. 2012; Pollack et al. 2016). Conceivably, the shock induced turbulence in the jets of BAL quasars is not strong enough to accelerate relativistic particles to the high energies needed for the emission of optical synchrotron radiation. Such a scenario would call for a more refined understanding of the physics of interaction of the inner relativistic jet with the rapidly outflowing BAL clouds of much denser thermal plasma, as envisioned in the polar model of BAL quasars (e.g., Ghosh & Punsly 2007). In parallel to such theoretical studies, it would also be worthwhile to intensify intranight optical monitoring of BAL–blazar candidates in sessions of longer durations.

ACKNOWLEDGMENTS

We thank the anonymous referee for the constructive comments on our manuscript. The scientific and technical staff of ARIES DFOT and ST are deeply acknowledged. Thanks are also due to the staff of IAO (Hanle) and CREST (Hosakote), for making possible a part of the observations reported here. The facilities at IAO and CREST are operated by the Indian Institute of Astrophysics, Bangalore. The valuable observing support provided by Ms. Raya Dastidar, Ms. Mridweeka Singh and Mr. Rakesh Pandey is also highly acknowledged.

REFERENCES

Becker R. H., White R. L., Gregg M. D., Brotherton M. S., Laurent-Muehleisen S. A., Arav N., 2000, *ApJ*, **538**, 72

Benn C. R., Carballo R., Holt J., Vigotti M., González-Serrano J. I., Mack K.-H., Perley R. A., 2005, *MNRAS*, **360**, 1455

Brotherton M. S., De Breuck C., Schaefer J. J., 2006, *MNRAS*, **372**, L58

Bruni G., et al., 2012, *A&A*, **542**, A13

Bruni G., Dallacasa D., Mack K.-H., Montenegro-Montes F. M., González-Serrano J. I., Holt J., Jiménez-Luján F., 2013, *A&A*, **554**, A94

Bruni G., Mack K.-H., Montenegro-Montes F. M., Brienza M., González-Serrano J. I., 2015, *A&A*, **582**, A9

Cohen M. H., Ogle P. M., Tran H. D., Vermeulen R. C., Miller J. S., Goodrich R. W., Martel A. R., 1995, *ApJ*, **448**, L77

Doi A., et al., 2009, *PASJ*, **61**, 1389

Elvis M., 2000, *ApJ*, **545**, 63

Fugmann W., 1988, *A&A*, **205**, 86

Ghosh K. K., Punsly B., 2007, *ApJ*, **661**, L139

Goodrich R. W., Miller J. S., 1995, *ApJ*, **448**, L73

Gopal-Krishna Wiita P. J., 2018, *Bulletin de la Societe Royale des Sciences de Liege*, **87**, 281

Gopal-Krishna Goyal A., Joshi S., Karthick C., Sagar R., Wiita P. J., Anupama G. C., Sahu D. K., 2011, *MNRAS*, **416**, 101

Goyal A., Gopal-Krishna Wiita P. J., Anupama G. C., Sahu D. K., Sagar R., Joshi S., 2012, *A&A*, **544**, A37

Goyal A., Gopal-Krishna Paul J. W., Stalin C. S., Sagar R., 2013, *MNRAS*, **435**, 1300

Gregg M. D., Becker R. H., de Vries W., 2006, *ApJ*, **641**, 210

Hall P. B., et al., 2002, *ApJS*, **141**, 267

Hamann F., Chartas G., Reeves J., Nardini E., 2018, *MNRAS*, **476**, 943

Hayashi T. J., Doi A., Nagai H., 2013, *ApJ*, **772**, 4

Hodge M. A., Lister M. L., Aller M. F., Aller H. D., Kovalev Y. Y., Pushkarev A. B., Savolainen T., 2018, *ApJ*, **862**, 151

Jiang D. R., Wang T. G., 2003, *A&A*, **397**, L13

Joshi R., Chand H., 2013, *MNRAS*, **429**, 1717

Kunert-Bajraszewska M., Cegłowski M., Katarzyński K., Roskowiński C., 2015, *A&A*, **579**, A109

Lister M. L., Smith P. S., 2000, *ApJ*, **541**, 66

Marscher A. P., et al., 2008, *Nature*, **452**, 966

Montenegro-Montes F. M., Mack K.-H., Vigotti M., Benn C. R., Carballo R., González-Serrano J. I., Holt J., Jiménez-Luján F., 2008, *MNRAS*, **388**, 1853

Murray N., Chiang J., Grossman S. A., Voit G. M., 1995, *ApJ*, **451**, 498

Pâris I., et al., 2012, *A&A*, **548**, A66

Pollack M., Pauls D., Wiita P. J., 2016, *ApJ*, **820**, 12

Prabhu T. P., Anupama G. C., 2010, in *Astronomical Society of India Conference Series*.

Proga D., Stone J. M., Kallman T. R., 2000, *ApJ*, **543**, 686

Punsly B., 1999, *ApJ*, **527**, 609

Romero G. E., Cellone S. A., Combi J. A., Andruchow I., 2002, *A&A*, **390**, 431

Sagar R., 1999, *Current Science*, **77**, 643

Sagar R., et al., 2011, *Current Science*, **101**, 1020

Stetson P. B., 1987, *PASP*, **99**, 191

Weymann R. J., Morris S. L., Foltz C. B., Hewett P. C., 1991, *ApJ*, **373**, 23

Yang J., Wu F., Paragi Z., An T., 2012, *MNRAS*, **419**, L74

Zhou H., Wang T., Wang H., Wang J., Yuan W., Lu Y., 2006, *ApJ*, **639**, 716